The Journal of Chemical Physics

RESEARCH ARTICLE | DECEMBER 28 2023

Studying the first order hyperpolarizability spectra in chalcone-based derivatives and the relation with one- and two-photon absorption transitions

Lucas F. Sciuti ; Carlos H. D. dos Santos ; Leandro H. Z. Cocca ; André G. Pelosi ; Rafaela G. M. da Costa ; Jones Limberger ; Cleber R. Mendonça ; Leonardo De Boni

J. Chem. Phys. 159, 244311 (2023)
https://doi.org/10.1063/5.0166036

The Journal of Chemical Physics ARTICLE pubs.aip.org/aip/jcp

Studying the first order hyperpolarizability spectra in chalcone-based derivatives and the relation with one- and two-photon absorption transitions

Cite as: J. Chem. Phys. 159, 244311 (2023); doi: 10.1063/5.0166036
Submitted: 2 July 2023 • Accepted: 6 December 2023 •
Published Online: 28 December 2023

Lucas F. Sciuti,[1] Carlos H. D. dos Santos,[1] Leandro H. Z. Cocca,[1] André G. Pelosi,[1] Rafaela G. M. da Costa,[2] Jones Limberger,[2] Cleber R. Mendonça,[1] and Leonardo De Boni[1,a)]

AFFILIATIONS

[1] São Carlos Institute of Physics, University of São Paulo, São Carlos, 13560-970 São Paulo, Brazil
[2] Departamento de Química, Pontifícia Universidade Católica do Rio de Janeiro, Rua Marquês de São Vicente, 225, 22451-900 Rio de Janeiro, Brazil

[a)] **Author to whom correspondence should be addressed:** deboni@ifsc.usp.br

ABSTRACT

The first-order molecular hyperpolarizability (β) dispersion was measured in seven chalcone-based molecules utilizing the tunable femtosecond hyper-Rayleigh scattering (tHRS) technique. Additionally, a theoretical model based on photophysical parameters was employed to better understand β dispersion. Due to the distinct substitution patterns of the aryl/heteroaryl rings within the chalcone structure, varying profiles of one- and two-photon absorption spectra and β dispersion were observed. The applied model highlighted two important factors contributing to achieving high β values: (i) the presence of red-shifted one-photon and two-photon absorption bands; and (ii) the number of discernible absorption bands. To contextualize these results with other molecular structures, we employed the HRS figure of merit (FOM). Remarkably, it was revealed that chemically engineered small chalcone molecules exhibit a FOM comparable to larger quadrupolar and octupolar ones. This underscores the significance of tHRS scattering measurements and their correlation with absorptive parameters in the design and characterization of nonlinear optical materials.

I. INTRODUCTION

In a nonlinear optical medium, the induced dipole moment is typically expressed using a series expansion in powers of the applied electric field.[1] The response of the electron distribution proportional to the squared electric field is denoted as the first-order molecular hyperpolarizability (β).[2] Therefore, knowledge of β is essential for guiding the design of new materials for nonlinear photonics and optoelectronic devices.[3,4] However, most studies on measuring β are conducted at a fixed wavelength, usually employing the Hyper-Rayleigh Scattering (HRS)[5] technique or the Electric-Field Induced Second Harmonic Generation (EFISHG)[6] method. Single-wavelength measurements of first-order molecular hyperpolarizability have supported the theoretical expectations. For instance, electron-withdrawing (EW) and electron-donating (ED) groups have already been demonstrated to enhance β values.[7,8] V-shaped and Y-shaped molecules also have high values of β due to an increase in the effective number of π-electrons and higher charge transfer induced at the excited states.[9,10] Although the knowledge of β in a single wavelength may be useful to indicate a compound as a candidate for nonlinear optical devices,[11–13] knowing the dispersion of β can provide insights to take advantage of enhanced effects in specific wavelength ranges as well as to target β values in a desired wavelength by molecular engineering. Research on measuring molecular $\beta(\lambda)$ has only been conducted over the past decade, primarily due to experimental challenges.[14–18] Nonetheless, those works showed that the dispersion of β leads to a deeper comprehension of the hyperpolarizability values and the electronic contributions that account for such dispersion.

A fascinating molecular category that could benefit from measuring β dispersion is the class of chalcone-based molecules. Chalcones refer to α, β-unsaturated ketones with aryl groups

attached to both the carbonyl group and the β-carbon. These molecules are widely observed in nature and can be easily synthesized from simple and readily available starting materials.[19] Synthetic chalcones have found broad applications across various fields, including biomedicine[20] (for cancer treatment, diabetes, and inflammation[21]) and opto-electronics.[22] One notable aspect of chalcones is the ease with which their optical properties can be modulated by simply altering the groups bonded to the peripheral aryl rings. Such structural modifications can significantly alter both the linear and nonlinear optical properties of these materials.[23,24] This alteration can drastically affect the one and two-photon electronic absorption, consequently impacting the dispersion of the first-order molecular hyperpolarizability.

Therefore, this work represents significant progress in understanding the fundamental structure-property relationship, mainly in second-order nonlinear effects. The research involved the measurement of one-photon absorption (1PA), two-photon absorption (2PA), and the spectral dependence of the first-order molecular hyperpolarizability (β). It delved into analyzing how the photophysical parameters governing the absorptive effect could offer insights into the dispersion of first-order molecular hyperpolarizability. Furthermore, the study employed phenomenological models that effectively described $\beta(\lambda)$, showcasing remarkable agreement when applied to the frequency-resolved Hyper-Rayleigh Scattering (HRS) data obtained.

II. EXPERIMENTAL DETAILS

This study involved measuring the linear and nonlinear absorption as well as the dispersion of the first-order molecular hyperpolarizability of seven chalcone-based molecules denoted as C1 to C7, with their molecular structures depicted in Fig. 1. Details regarding the synthesis of these compounds can be found in Refs. 19 and 25. All samples were dissolved in pure dimethyl sulfoxide (DMSO). The variation among the chalcone-based molecules lies in their peripheral groups. The chalcones (C1–C7) examined here have distinct substitution patterns, as illustrated in Fig. 1. C1 represents the non-substituted pattern. On the other hand, C2 and C3 feature substitutions solely in the benzaldehyde ring (A position), with C2 containing an electron-withdrawing fluorine atom and C3 possessing a highly electron-donating NH2 group, both situated at the *para* position. In the case of C4 and C5, substitutions were introduced on both aryl rings. C4 exhibits two methoxy groups, while C5 has one methoxy group and a chlorine atom. As for C6 and C7, the former is a bromo-substituted chalcone, while the latter displays a furane in ring B and a chloroarene at the benzaldehyde ring.

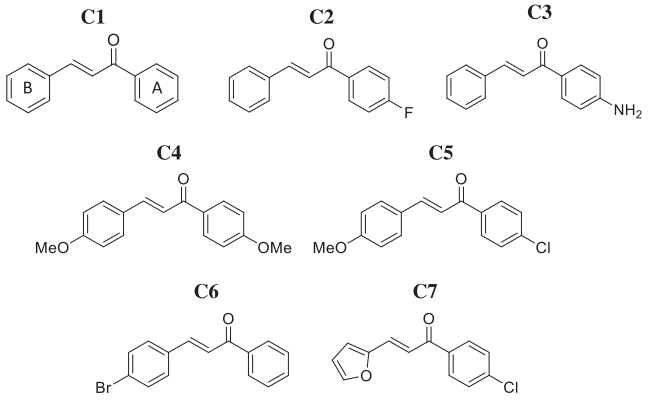

FIG. 1. Seven (C1 to C7) chalcone-based molecule structures used in this work. The letters A and B in molecule C1 represent the two aromatic rings that are commonly found in chalcone-based molecules.

A. One- and two-photon absorption measurement

One-photon absorption measurements were performed using a commercial SHIMADZU UV-1800 spectrometer. All molecules were dissolved in pure DMSO at concentrations of ~10^{-4} mol/l. These measurements provided insights into the central frequency (ω_{0n}) and linewidth (γ_{0n}) of transitions from the electronic ground state ($n = 0$) to various excited states ($n = 1, 2, 3 \ldots$). For the two-photon absorption (2PA) measurements, a tunable femtosecond open aperture Z-scan technique was employed. This technique utilized an amplified Ti:Sapphire laser (CPA-2001 system from Clark-MXR) emitting pulses centered at 775 nm with a temporal width of 120 fs and a repetition rate of 1 kHz. It pumped an Optical Parametric Amplifier (OPA) (TOPAS—Quantronix) that produced pulses within a spectral range of 460–2000 nm. Further technical details can be found elsewhere.[26,27] Details of the experimental setup and examples of Z-scan signatures obtained in this work are presented in Sec. 1 of the supplementary material. The Sum Over Essential States (SOES) model was used to adjust the 2PA cross-section spectra, $\sigma_{2PA}(\lambda)$. This adjustment utilized two key photophysical parameters: the transition dipole moment between the molecular electronic states m and n (μ_{nm}) and the difference between the permanent dipole moments of two molecular electronic states ($\Delta\mu_{nm}$).

B. Tunable femtosecond HRS technique

To obtain the dispersion of the first order molecular hyperpolarizability, a tunable femtosecond HRS technique was employed. It consists of an optical parametric amplifier (Orpheus—Light Conversion) pumped by an amplified femtosecond laser system (Pharos—Light Conversion, 1030 nm, 190 fs, 7.5 kHz) as the tunable laser excitation, allowing wavelength tuning from visible to near-infrared. A detailed description of the experimental apparatus can be found elsewhere.[28] For a given laser output frequency ω, a typical curve of the incoherent scattered second harmonic signal, $I(2\omega)$, is obtained as a function of incident beam intensity $I(\omega)$. The determination of $\beta(\lambda)$ is performed through the External Reference Method (ERM).[5] Examples of ERM experimental curves as a function of the sample concentrations are shown in Sec. 2 of the supplementary material. Furthermore, it was assumed that all studied molecules exhibited C2v-like symmetry (depolarization ratio $\rho = \langle\beta^2_{XZZ}\rangle/\langle\beta^2_{ZZZ}\rangle = 1/5$), in which the most uniaxial dipolar molecules had the z-axis as the molecular dipole axis, and consequently, the βzzz component was much larger than βzxx.[29,30] The reference sample was para-nitroaniline (pNA) dissolved in pure

DMSO. The expected quadratic coefficient between $I(2\omega)$ and $I(\omega)$ is measured in different concentrations for both the studied and reference molecules. The concentrations of the samples and the reference were in the range of 10^{-2}M to 10^{-3}M. $\beta(\lambda)$ is obtained by the ratio between the linear behavior of the quadratic coefficient as a function of the concentration of both the measured molecule and the reference molecule, based on the *a priori* knowledge of the reference molecule $\beta_{ref}(\lambda)$. Additional details of ERM can be found in Refs. 16 and 28. The fundamental equation and examples of the experimental curves are in the supplementary material, Sec. 2. It is important to note that none of the samples exhibited any fluorescence induced by one- and two-photon absorption, including the reference sample.

III. RESULTS AND DISCUSSIONS

Figure 2 shows the measurements of one and two-photon absorption cross-section spectra. The dashed red lines indicate the molar absorptivity coefficient, measured from 245 to 455 nm. As expected, the chalcone molecule (C1) has a low energy band around 315 nm, resulting in a transition dipole moment from the ground to the first electronic excited state (μ_{01}) of around 6.3 D, which is also

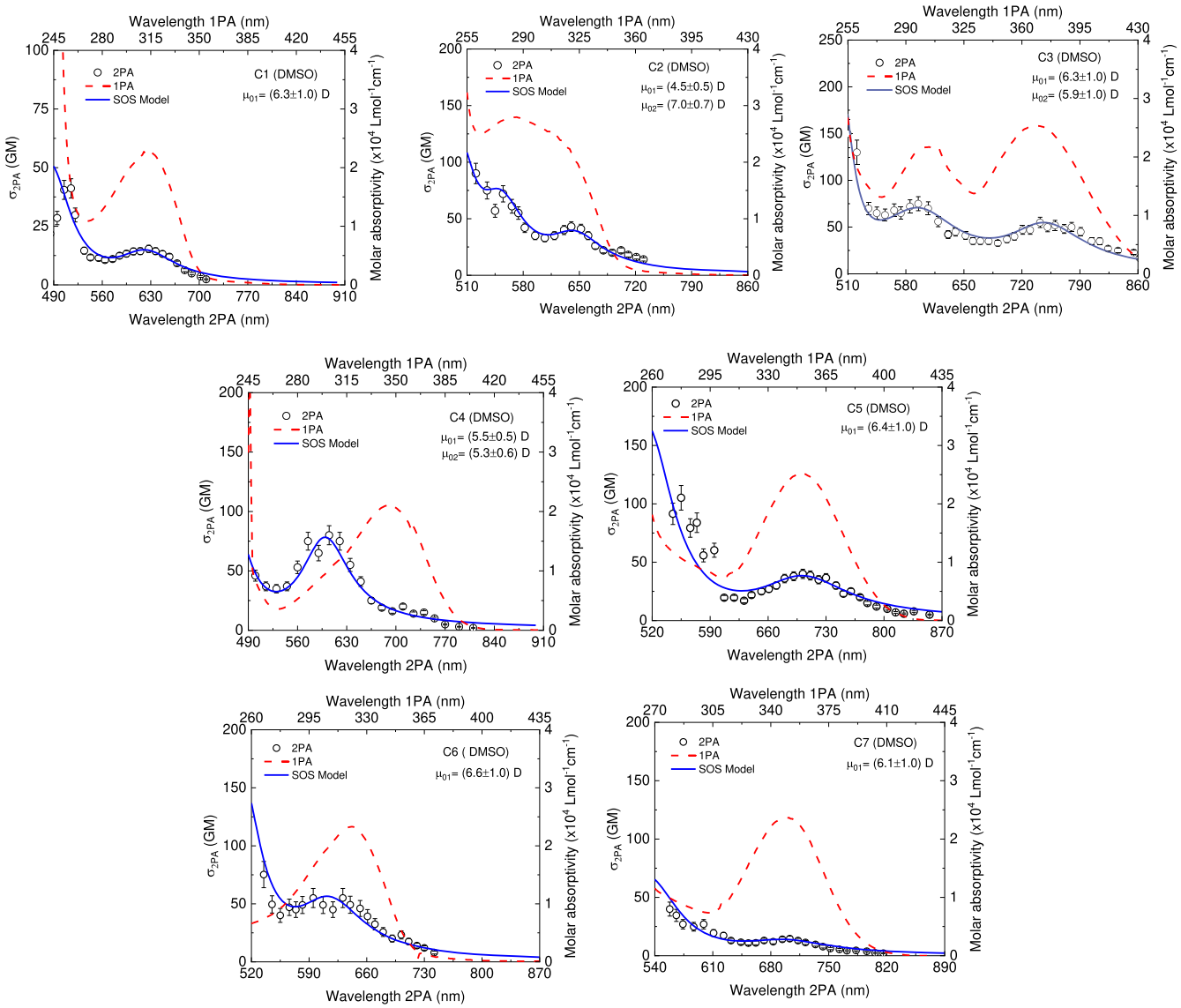

FIG. 2. One- (dashed red lines) and two-photon (open black circles) absorption spectra of the seven chalcone-based molecules. Transition dipole moments are displayed on the insets in Debye units. The fitting of the sum-over-state model on the experimental two-photon absorption cross-sections is displayed in solid blue lines. The error bars concerting the experimental two-photon absorption cross-sections are related to sample concentration and laser power fluctuation estimated at 10%.

in concordance with values already reported.[16] All molecules studied in this work displayed electronic absorption bands with (μ_{01}) values between 4.5 D and 7.0 D, which agrees with previously reported chalcone-based molecules.[7,24,31–34] The molecule C2 exhibits its lowest energy band around 315 nm, similar to C1, but also shows a second higher energy band around 280 nm, which differs from C1. This difference may be attributed to the presence of the fluorine atom in aromatic ring A. For C3, the fluorine is substituted by an amine group. As seen in the C3 chart, the amine group causes a red-shift in the lower energy band, resulting in a notable displacement compared to C1, ~0.46 eV. This shift is expected due to the NH_2 group, which acts as an electron donor and causes an increase in the highest occupied molecular orbital (HOMO). Consequently, this results in a reduction in the energy gap between the HOMO and the lowest unoccupied molecular orbital (LUMO).[35,36] Molecules C4 and C5 have similar absorption bands with a 0.32 eV red-shift compared to the lower energy band of C1. It is caused by the methoxy attached to the B aromatic ring. The shoulders at 290 nm for C4 and 280 nm for C5 represent the high energy band red-shifted, similar to C2, caused by the presence of the methoxy and chlorine attached to aromatic ring A. In the case of molecule C6, its absorption spectrum closely resembles that of molecule C1, suggesting that the bromine atom has a minimal impact on this particular molecular property. Finally, molecule C7 also displays a red-shifted absorption band compared to C1, primarily due to the presence of the furan group.[37,38]

Regarding the 2PA experimental spectra illustrated in Fig. 2 (depicted as open circles), most of the molecules exhibited a 2PA band occurring at twice the wavelength of 1PA, as anticipated for non-centrosymmetric molecules, such as those studied in this work. Some examples of open aperture Z-scan technique signatures can be found in section 1 of the supplementary material. The 2PA maxima ranged from about 20 GM (for molecules C1 and C7) to 80 GM (for molecule C4). On the 2PA experimental data, we employ the SOS approach to extract the values of the difference between the permanent dipole moments of the ground and first excited state, the ground and the second excited state, and the transition dipole moment between the first and second excited states, respectively, $\Delta\mu_{01}$, $\Delta\mu_{02}$, and μ_{12} for all the molecules studied. The 2PA cross-section spectrum for a non-centrosymmetric charge distribution (solid blue lines in Fig. 2) can be described through the following expression:

$$\sigma_{2PA}(\omega) = \frac{2}{5}\frac{(2\pi)^5}{(chn)^2}L^4\frac{1}{\pi}\left[\frac{\Delta\mu_{01}^2\mu_{01}^2\Gamma_{01}}{(\omega_{01}-2\omega)^2+\Gamma_{01}^2}+\frac{\Delta\mu_{02}^2\mu_{02}^2\Gamma_{02}}{(\omega_{02}-2\omega)^2+\Gamma_{02}^2}+\frac{\omega^2}{(\omega_{01}-\omega)^2+\Gamma_{01}^2}\frac{\mu_{12}^2\mu_{01}^2\Gamma_{02}}{(\omega_{02}-2\omega)^2+\Gamma_{02}^2}+\frac{\Delta\mu_{02}\mu_{02}\mu_{01}\mu_{12}\Gamma_{02}}{(\omega_{02}-2\omega)^2+\Gamma_{02}^2}\right], \quad (1)$$

in which h is Planck's constant, c is the speed of light, n is the DMSO linear refractive index (n = 1.4793), and L is the Onsager's local field factor given by $L = 3n^2/(2n^2+1)$. The damping factors (Γ_{nm}) used were about 0.4 eV. All the terms inside the square brackets were used to describe the first 2PA absorption band (first term), the second 2PA absorption (second term), the 1PA enhancement effect (third term), and the interference term between both excited states (fourth term). The complete equation [Eq. (1)] was used to model the 2PA spectrum for molecules C2, C3, and C4, while to model C1, C5, C6, and C7, only the first term in Eq. (1) was used due to the presence of only one 2PA band. All the photophysical parameters obtained through the one- and two-photon absorption spectra are displayed in Table I.

The 1PA and 2PA spectra of chalcone-based molecules have also been extensively studied in terms of quantum chemistry calculations (QCC). For instance, a recent study[33] calculated QCC for second and third-order nonlinearities in non-substituted chalcone molecules (as C1 in this work). It was shown that QCC predicts a single central electronic transition at 312 nm in methanol, which is similar to our case of C1 in DMSO. The differences in the solvent used could indicate a low solvent-related shift. The study also provided QCC for a methoxy mono-substituted chalcone, similar to C4 in this work, which contains methoxy groups attached to both aromatic rings, and their QCC results showed two absorption bands with relatively high oscillator strength: f = 0.958 at 337 nm and f = 0.186 at 252 nm. In Table I, the values of λ_{01} and λ_{02} for C4 show a redshift of both absorption bands, which could be associated with the second methoxy group present in C4. Other recent works[7,24,34,39] have also calculated the electronic density of the HOMO and the LUMO for chalcone-based molecules at the CAM-B3LYP functional in vacuum, dichloromethane (DCM), and DMSO medium. Manoel *et al.*[24] used the QCC of two experimentally obtained absorption bands of chalcone-based molecules to demonstrate that the lowest

TABLE I. Photophysical parameters obtained from one- and two-photon absorption spectra and from the output of the SOS model. λ_{01} and λ_{02} are the central wavelengths of each absorption band. μ_{01} and μ_{02} were obtained through the one-photon absorption spectra. $\Delta\mu_{01}$, $\Delta\mu_{02}$, and μ_{12} were obtained by fitting the SOS model to the two-photon absorption spectra.

	C1	C2	C3	C4	C5	C6	C7
λ_{01} (nm)	314	323	370	350	352	323	350
μ_{01} (D)	6 ± 1	4.5 ± 0.5	6.3 ± 0.7	5.5 ± 0.5	6 ± 1	7 ± 1	6 ± 1
$\Delta\mu_{01}$ (D)	7 ± 1	12 ± 1	12 ± 1	6.0 ± 0.5	12 ± 1	13 ± 1	6 ± 1
λ_{02} (nm)	⋯	277	303	306	⋯	⋯	⋯
μ_{02} (D)	⋯	7.0 ± 0.7	5.9 ± 0.6	5.3 ± 0.5	⋯	⋯	⋯
$\Delta\mu_{02}$ (D)	⋯	8.5 ± 0.9	13 ± 2	16 ± 2	⋯	⋯	⋯
μ_{12} (D)	9 ± 1	5.0 ± 0.6	4.2 ± 0.5	5.5 ± 0.6	14 ± 2	14 ± 2	9 ± 1

energy band originates mainly due to the HOMO-LUMO transition corresponding to a π–π^* excited state.

The first order molecular hyperpolarizability dispersion can be modeled using the SOS, in which the well-known two-level model (2LM) and three-level model (3LM) were used in this work. Those models are the result of several extensive studies that search for ways to model both first and second order hyperpolarizabilities.[40–43] The main challenge is to deal with the balance of a nonrealistic simple model or a complex model that involves a large number of photophysical parameters that become nonrealistic when determined experimentally. The 2LM and 3LM are special cases of those solutions considering the ground and one excited state, or the ground and the two excited states, respectively. For instance, based on the complete solution from Sciuti *et al.*,[16] the functional can be written as

$$\begin{aligned}\beta_{3LM}(\omega,\omega_{01},\omega_{02},\Gamma_{01},\Gamma_{02}) &= \beta_{2LM}(\omega,\omega_{01},\Gamma_{01}) + \left[\frac{3}{2}\frac{\mu_{01}\mu_{12}\mu_{02}}{(\hbar\omega_{01})(\hbar\omega_{02})}\right] \\ &\times\left[\left(\frac{1}{3}\frac{\omega_{01}}{[(\omega_{01}-2\omega)-i\Gamma_{01}]}\frac{\omega_{02}}{[(\omega_{02}-\omega)-i\Gamma_{02}]}\right)\right] \\ &+\left[\frac{3}{2}\frac{\mu_{02}^2\Delta\mu_{02}}{(\hbar\omega_{02})^2}\right]\left[\left(\frac{1}{3}\frac{\omega_{02}}{[(\omega_{02}-2\omega)-i\Gamma_{02}]}\right.\right. \\ &\times\left.\left.\frac{\omega_{02}}{[(\omega_{02}-\omega)-i\Gamma_{02}]}\right)\right], \end{aligned} \tag{2}$$

$$\beta_{2LM}(\omega,\omega_{01},\Gamma_{01}) = \left[\frac{3\mu_{01}{}^2\Delta\mu_{01}}{2(\hbar\omega_{01})^2}\right]\left[\left(\frac{1}{3}\frac{\omega_{01}}{[(\omega_{01}-\omega)-i\Gamma_{01}]}\right.\right. \times\left.\left.\frac{\omega_{01}}{[(\omega_{01}-2\omega)-i\Gamma_{01}]}\right)\right], \tag{3}$$

where the static (β_0) and dynamic first order molecular hyperpolarizability terms are in the first and second squared brackets, respectively. In the absence of the second higher electronic band (2LM), the second and third terms will cancel. It is worth noting that Eq. (2) is a simplified model of the one found in Sciuti *et al.*[16] The anti-resonant terms for $\beta(\omega)$ were disregarded due to their significantly low contribution values within the measured spectral region, falling well below the confidence interval. This decision was made after considering the experimental errors associated with the photophysical parameters. Further details can be found elsewhere.[28] In this context, β_0 dictates the dispersion of the first order scattering nonlinear response when $\omega \to 0$, which depends on the transition dipole moment from two electronic states (μ_{01}), the difference between the permanent dipole moment ($\Delta\mu_{01}$) of the ground and the first electronic excited state, and the energy gap between those two states ($\hbar\omega_{01}$). The second squared bracket is the dynamical component, encompassing one- and two-photon resonance terms. A careful analysis of this term reveals that it governs the dispersion of β with the maxima located where the two terms in the denominator approach zero, i.e., when the incident light frequency is equal to half of the resonance frequency of the molecule. Therefore, if just one experimentally observed absorption band is observed at the UV–Vis region, $\beta(\lambda)$ can be accurately modeled by Eq. (3), as is the case for molecules C1, C5, C6, and C7.

In the case of C2, C3, and C4, where two excited states were experimentally observed within the UV–Vis region, both states might contribute to $\beta(\lambda)$. Therefore, if this is the case, one can accurately model the β dispersion using the 3LM. As observed in Eq. (2), the β value for the 3LM possesses the 2LM dispersion and two additional terms: the first one is due to the dipole moment from the first and second excited states, while the second term is due to the dipole moment between the ground and second excited states.

Equation (2) demonstrates that the dispersion of the first molecular hyperpolarizability relies on photophysical parameters that can be derived from 1PA and 2PA experiments. Therefore, based on the 1PA and 2PA measurements already described for the seven chalcone-based molecules, it is possible to calculate the $\beta(\lambda)$. As previously mentioned, we also experimentally measured $\beta(\lambda)$ to validate the effectiveness of 2LM and 3LM to accurately predict a sometimes challenging-to-measure first order scattering parameter.

Both the experimental and the model of $\beta(\lambda)$ are depicted in Fig. 3, respectively, as black circles and black lines. As one can notice, the experimental points were measured from 750 to 1064 nm, and the values at 1064 nm are comparable to similar molecules reported in the literature.[7,28,44,45] The model-generated curve confidence interval (gray shade in Fig. 3) is due to experimental uncertainties of the photophysical input parameters to the model. The experimental data and the model are in accordance, mainly for longer wavelengths. Molecules C2, C3, and C4 have two experimentally observed absorption bands; therefore, they are modeled with 3LM to take into account both bands, which reflects the broader first order molecular hyperpolarizability dispersion.

As a first step in analyzing $\beta(\lambda)$, the dispersion can be extrapolated when the excitation energy approaches zero ($\lambda \to \infty$), referred to as the static first order hyperpolarizability (β_0). Table II presents these values for the chalcone-based molecules, which are aligned with similar molecules previously reported in the literature.[24,33,46] Using the C1 molecule as the baseline reference for β_0, it is evident that the β_0 value increases by almost five times for the C3 molecule. This heightened β_0 value is associated with the presence of the second absorption band at the UV–Vis region, represented by the second and third terms in Eq. (2), as well as the red-shift of the first absorption band when compared to the other molecules. The higher values of C5 and C6 compared to C1 and C7 are related to the highest μ_{01} values. Lastly, the C1 and C7 molecules have similar photophysical parameter values; however, C7 shows a considerable red shift concerning the lower energy absorption band (~40 nm), resulting in a 20% increase in β_0 values.

To shed light on the $\beta(\lambda)$ responses between 2LM and 3LM molecular systems, Fig. 4 shows the $\beta(\lambda = 1064\ \text{nm})$ concerning the lowest energy absorption band maximum wavelength. As it can be seen, the molecule absorption band with lower transition energy (longer wavelength) tends to increase the $\beta(\lambda = 1064\ \text{nm})$ (as indicated by the blue circles and blue dashed line). This same trend is observed for molecules exhibiting two absorption bands (as denoted by the orange circles and orange dashed lines). A more pronounced effect is the difference in the β values in molecules with one and two absorption bands. For instance, despite the fact that C7 has a longer absorption maximum wavelength than C2, the presence of two absorption bands in C2 results in its $\beta(\lambda = 1064\ \text{nm})$ being

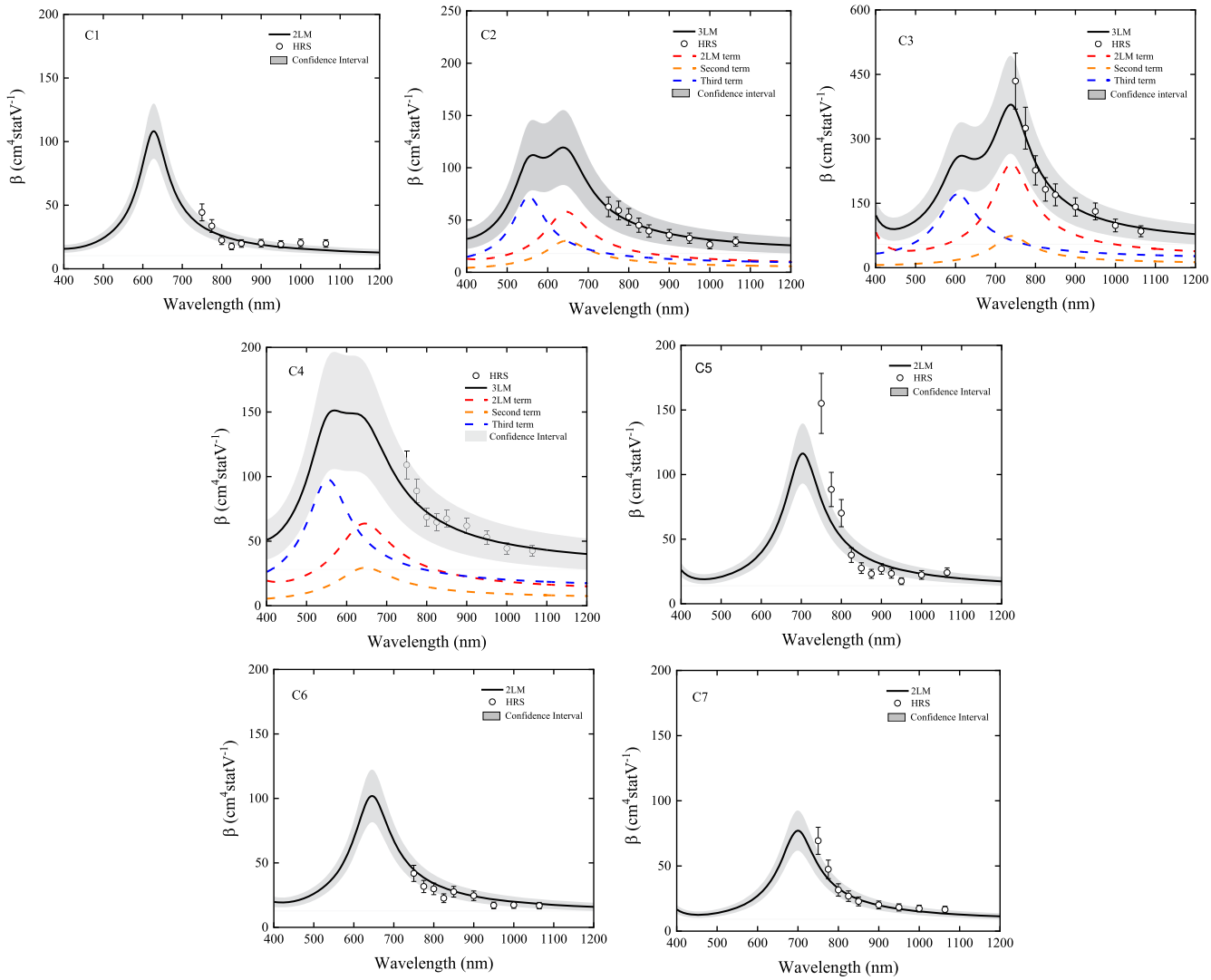

FIG. 3. First molecular hyperpolarizability dispersion $\beta(\lambda)$ calculated using Eqs. (2) and (3) (black solid lines) and the, respectively, calculated confidence interval, associated with the standard deviation of the experimentally measured photophysical parameters (gray shade). The open black circles are the experimentally measured data using the HRS technique. Dashed lines in C2, C3, and C4 are three components of Eq. (2) being highlighted: the 2LM in red, the second term in orange, and the third term in blue.

TABLE II. First-order static hyperpolarizability (β_0) for molecules C1 to C7. The blue and red colors in the molecule names are associated with 2LM and 3LM modeling, respectively.

Molecules	C1	C2	C3	C4	C5	C6	C7
β_0 (cm^4 statV^{-1})	10 ± 3	17 ± 3	46 ± 9	16 ± 3	22 ± 4	22 ± 4	12 ± 2

almost twice as high as that of C7. This can be verified by analyzing Eqs. (2) and (3). The presence of the second absorption band in certain molecules introduces two additional terms in the static first order hyperpolarizability, contributing to an increased $\beta(\lambda)$ for C2 when compared to C7.

Hence, in general, a stronger lower-energy absorption band corresponds to a higher value of β, as described in Eq. (2). This change rate can be seen as the slope of the dashed blue line in Fig. 4. However, the rate of change in β also occurs for molecules with two absorption bands, but at a higher rate, which can be visualized as the slope of the dashed orange line in Fig. 4. This happens for two reasons: firstly, due to the additional two terms in the static first-order hyperpolarizability arising from the second absorption band, and secondly, because both absorption bands are red-shifted, as in the case of C3 compared to C2. This principle should hold for another set of molecules, offering a potential new pathway for discovering small molecules with high nonlinearities in the sense that molecular engineering for high values of β for small molecules could be better achieved by attaching molecular groups that create a

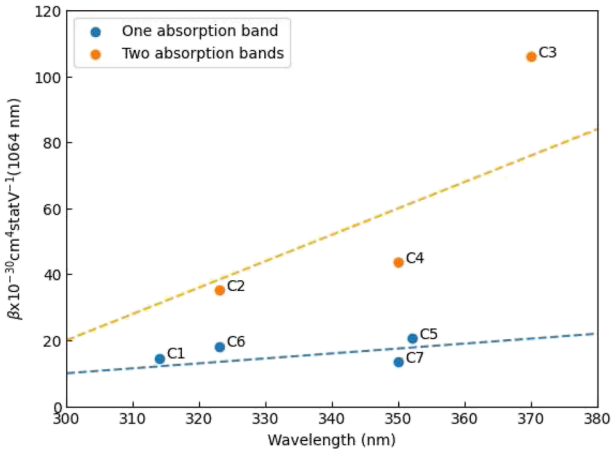

FIG. 4. The first molecular hyperpolarizability is presented as a function of the lowest energy absorption band central wavelength. Blue circles represent molecules exhibiting only one experimentally observed absorption band, whereas orange circles depict molecules with two experimentally observed absorption bands. The dashed lines are provided solely as visual guides.

second electronic energy band as redshifted as possible rather than just red-shifting two-level system molecules.

Molecule C3 has the highest value of $\beta(\lambda = 1064\ \text{nm})$ mainly because it has the two features that enhance the effect, i.e., the most red-shifted one- and two-photon absorption bands and the presence of two absorption bands and, therefore, the 3LM is necessary for accurately model β dispersion. To compare the value of $\beta(\lambda = 1064\ \text{nm})$ of C3 with other molecules already reported, we employed the first molecular hyperpolarizability figure of merit, $FOM = \beta(1064\ \text{nm})/N_{eff}^{3/2}$, where N_{eff} is the effective number of π-conjugated electrons, calculated as twice the number of double and triple bounds.[47,48] For C3, $N_{eff} = 14$, consequently, $FOM_{C3} = (2.0 \pm 1.0) \times 10^{-30}$ cm^4 statV^{-1}. Cesaretti *et al.*[49] studied small molecules with high values of β by engineering molecules as cationic push-pull systems. They managed to achieve $FOM(\beta_0) = 3.1 \times 10^{-30}$ cm^4 statV^{-1} with a molecule that also has NH_3 as a peripheral group (similar to the C3 molecule) and using DCM as a solvent. Notably, DCM significantly redshifted the absorption dispersion, akin to how molecule C3 displayed the most redshifted lowest absorption energy band. Abegão *et al.*[7] investigated chalcone-based molecules incorporating acetophenone as peripheral structures. They utilized DCM as the solvent, a choice known to favor redshift, as shown in Ref. 40, and consequently, increase β_0. Their highest β_0 molecule achieved $FOM(\beta(1064\ \text{nm})) = 0.72 \times 10^{-30}$ cm^4 statV^{-1} with $N_{eff} = 14$, the same as C3, but C3 had $\beta(1064\ \text{nm})$ almost three times higher. Finally, Fonseca and colleagues[10] studied the first-order hyperpolarizability of V- and Y-shaped molecules. The Y-shaped molecules, with $N_{eff} = 48$, resulted in $FOM(\beta(1064\ \text{nm})) = 2.7 \times 10^{-30}$ cm^4 statV^{-1}, just 35% higher than molecule C3. This demonstrates that despite the fact that chalcone-based molecules are considered small molecules, when appropriately engineered, they can present proportionally high values of the first molecular hyperpolarizability. Extensive work has been performed in this direction concerning third-order nonlinearities,[50,51] in which the molecular engineering strategy is also adding small functional groups to small molecules, aiming to decrease the energy distance between HOMO and LUMO.[52]

IV. FINAL REMARKS

One and two-photon absorption spectra were measured for seven chalcone-based molecules. Among these, C2, C3, and C4 exhibited two distinct 1PA bands within the UV–Vis spectral region, while C1, C5, C6, and C7 displayed only one in the same spectral region. Moreover, the first order hyperpolarizability was measured from 750 to 1064 nm through the tHRS technique, applying the external reference method. A photophysical parameter-based model was used to reproduce $\beta(\lambda)$. The dispersion of β revealed two important molecular characteristics responsible for increasing β for such molecules: the more red-shifted, the lower the energy band, and second, the number of excited states at the same spectral region of the nonlinear scattering.

Concerning the chalcone-based derivatives, it was found that molecule C3, possessing two excited states and featuring the most red-shifted lower absorption band, exhibited the highest value of $\beta(\lambda)$. Comparatively, when contrasted with the simplest chalcone molecule in this study, C1, the values were nearly nine times higher within the range of 750–900 nm. Even at 1064 nm, C3 also displayed the highest value, and by calculating the effective number of π-conjugated electrons, it was possible to show that the $FOM_{C3} = (2.0 \pm 1.0) \times 10^{-30}$ cm^4 statV^{-1} is comparable to that of quadrupolar and octupolar molecular systems, which are expected to present high values of the first-order molecular hyperpolarizability.

SUPPLEMENTARY MATERIAL

See the supplementary material for the details of the Z-scan technique with nonlinear absorption signatures and for the description of the External Reference Method (ERM) to calculate experimentally the β(λ) values.

ACKNOWLEDGMENTS

Financial support from FAPESP (Fundação de Amparo à Pesquisa do Estado de São Paulo, Grant Nos. 2011/12399-0, 2015/20032-0, 2016/20886-1, and 2018/11283-7), CNPq (Conselho Nacional de Desenvolvimento Científico e Tecnológico, Grant No. 425180/2018-2), Coordenação de Aperfeiçoamento de Pessoal de Nível Superior (CAPES) Finance Code 001, FAPERJ (Fundação de Amparo à Pesquisa do Estado do Rio de Janeiro, Grant Nos. SEI-26/0003/001526/2022, SEI-260003/015152/2021, and SEI-26/0003/001608/2022), Army Research Laboratory (Grant No. W911NF2110362) and Air Force Office of Scientific Research (Grant No. FA9550-12-1-0028) are acknowledged.

AUTHOR DECLARATIONS

Conflict of Interest

The authors have no conflicts to disclose.

Author Contributions

Lucas F. Sciuti: Conceptualization (equal); Data curation (equal); Investigation (equal); Methodology (equal); Writing – original draft (equal); Writing – review & editing (equal). **Carlos H. D. dos Santos**: Investigation (equal); Validation (equal); Writing – review & editing (equal). **Leandro H. Z. Cocca**: Formal analysis (equal); Investigation (equal); Validation (equal); Writing – review & editing (equal). **André G. Pelosi**: Investigation (equal). **Rafaela G. M. da Costa**: Resources (equal). **Jones Limberger**: Supervision (equal); Validation (equal); Writing – review & editing (equal). **Cleber R. Mendonça**: Supervision (equal); Validation (equal); Writing – review & editing (equal). **Leonardo De Boni**: Supervision (equal); Validation (equal); Writing – review & editing (equal).

DATA AVAILABILITY

The data that support the findings of this study are available from the corresponding author upon reasonable request.

REFERENCES

[1] R. Boyd, *Nonlinear Optics* (Elsevier, 2019).
[2] J. J. Wolff and R. Wortmann, "Organic materials for second-order non-linear optics," Adv. Phys. Org. Chem. **32**, 121–217 (1999).
[3] Y. Yan, Y. Yuan, B. Wang, V. Gopalan, and N. C. Giebink, "Sub-wavelength modulation of χ(2) optical nonlinearity in organic thin films," Nat. Commun. **8**, 14269 (2017).
[4] J. Liu, C. Ouyang, F. Huo, W. He, and A. Cao, "Progress in the enhancement of electro-optic coefficients and orientation stability for organic second-order nonlinear optical materials," Dyes Pigm. **181**, 108509 (2020).
[5] K. Clays and A. Persoons, "Hyper-Rayleigh scattering in solution," Rev. Sci. Instrum. **63**, 3285 (1992).
[6] R. W. Terhune, P. D. Maker, and C. M. Savage, "Optical harmonic generation in calcite," Phys. Rev. Lett. **8**, 404 (1962).
[7] L. M. G. Abegão *et al.*, "Chalcone-based molecules: Experimental and theoretical studies on the two-photon absorption and molecular first hyperpolarizability," Spectrochim. Acta, Part A **227**, 117772 (2020).
[8] L. C. S. Nair, S. Balachandran, D. Arul Dhas, and I. Hubert Joe, "In-silico analysis of substituent effect on the static first order hyperpolarizability of electron donating mono substituted chalcone derivatives," J. Mol. Model. **24**, 126 (2018).
[9] M. G. Vivas *et al.*, "Molecular structure-optical property relationship of salicylidene derivatives: A study on the first-order hyperpolarizability," J. Phys. Chem. A **125**, 99–105 (2021).
[10] R. D. Fonseca *et al.*, "First-order hyperpolarizability of triphenylamine derivatives containing cyanopyridine: Molecular branching effect," J. Phys. Chem. C **122**, 1770–1778 (2018).
[11] M. Shkir *et al.*, "An investigation on the key features of a D–π–A type novel chalcone derivative for opto-electronic applications," RSC Adv. **5**, 87320–87332 (2015).
[12] D. Haleshappa *et al.*, "Structural, photoluminescence, physical, optical limiting, and hirshfeld surface analysis of polymorphic chlorophenyl organic chalcone derivative for optoelectronic applications," J. Mol. Struct. **1232**, 130053 (2021).
[13] S. J. Armaković, Y. S. Mary, Y. S. Mary, S. Pelemiš, and S. Armaković, "Optoelectronic properties of the newly designed 1,3,5-triazine derivatives with isatin, chalcone and acridone moieties," Comput. Theor. Chem. **1197**, 113160 (2021).
[14] Y. De Coene *et al.*, "Fluorescence-free spectral dispersion of the molecular first hyperpolarizability of bacteriorhodopsin," J. Phys. Chem. C **121**, 6909–6915 (2017).
[15] S. Van Cleuvenbergen *et al.*, "Dispersion overwhelms charge transfer in determining the magnitude of the first hyperpolarizability in triindole octupoles," J. Phys. Chem. C **116**, 12312–12321 (2012).
[16] L. F. Sciuti *et al.*, "Modeling the first-order molecular hyperpolarizability dispersion from experimentally obtained one- and two-photon absorption," J. Phys. Chem. A **126**, 2152–2159 (2022).
[17] J. Campo, A. Painelli, F. Terenziani, T. Van Regemorter, D. Beljonne, E. Goovaerts, and W. Wenseleers, J. Am. Chem. Soc. **132**(46), 16467–16478 (2010).
[18] J. Campo, W. Wenseleers, J. M. Hales, N. S. Makarov, and J. W. Perry, "Accurate and practically implementable model for first hyperpolarizability dispersion," in *Latin America Optics and Photonics Conference* (Optica Publishing Group, 2012), p. LT2A.8.
[19] C. Zhuang *et al.*, "Chalcone: A privileged structure in medicinal chemistry," Chem. Rev. **117**, 7762–7810 (2017).
[20] D. K. Mahapatra, S. K. Bharti, and V. Asati, "Chalcone derivatives: Anti-inflammatory potential and molecular targets perspectives," Curr. Top. Med. Chem. **17**, 3146–3169 (2017).
[21] B. Salehi *et al.*, "Pharmacological properties of chalcones: A review of preclinical including molecular mechanisms and clinical evidence," Front. Pharmacol. **11**, 592654 (2021).
[22] M. K. M. Ali *et al.*, "Characterization of optical and morphological properties of chalcone thin films for optoelectronics applications," Optik **145**, 529–533 (2017).
[23] T. Andrade-Filho *et al.*, "Insights and modelling on the nonlinear optical response, reactivity, and structure of chalcones and dihydrochalcones," J. Mol. Struct. **1246**, 131182 (2021).
[24] D. S. Manoel *et al.*, "Second- and third-order nonlinear optical properties of mono-substituted terpenoid-like chalcones," J. Photochem. Photobiol., A **429**, 113898 (2022).
[25] R. G. M. da Costa, F. R. L. Farias, D. Back, and J. Limberger, "Synthesis of arylated chalcone derivatives via palladium cross-coupling reactions," Tetrahedron Lett. **59**, 771–775 (2018).
[26] M. Sheik-Bahae, A. A. Said, T. H. Wei, D. J. Hagan, and E. W. van Stryland, "Sensitive measurement of optical nonlinearities using a single beam," IEEE J. Quantum Electron. **26**, 760–769 (1990).
[27] D. S. Corrêa *et al.*, "Z-scan theoretical analysis for three-, four- and five-photon absorption," Opt. Commun. **277**, 440 (2007).
[28] C. H. D. Dos Santos *et al.*, "Observation of the two-photon transition enhanced first hyperpolarizability spectra in cinnamaldehyde derivatives: A femtosecond regime study," J. Chem. Phys. **158**, 214201 (2023).
[29] T. Verbiest, K. Clays, and V. Rodriguez, *Second-order Nonlinear Optical Characterization Techniques: An Introduction* (CRC Press, 2009).
[30] G. J. T. Heesink, A. G. T. Ruiter, N. F. Van Hulst, and B. Bölger, "Determination of hyperpolarizability tensor components by depolarized hyper Rayleigh scattering," Phys. Rev. Lett. **71**, 999–1002 (1993).
[31] J. M. F. Custodio *et al.*, "Chalcone as potential nonlinear optical material: A combined theoretical, structural, and spectroscopic study," J. Phys. Chem. C **123**, 5931–5941 (2019).
[32] R. G. M. da Costa *et al.*, "Synthesis, photophysical properties and aggregation-induced enhanced emission of bischalcone-benzothiadiazole and chalcone-benzothiadiazole hybrids," J. Lumin. **239**, 118367 (2021).
[33] L. M. G. Abegão *et al.*, "Second- and third-order nonlinear optical properties of unsubstituted and mono-substituted chalcones," Chem. Phys. Lett. **648**, 91–96 (2016).
[34] A. G. Pelosi *et al.*, "Two-photon absorption and multiphoton excited fluorescence of acetamide-chalcone derivatives: The role of dimethylamine group on the nonlinear optical and photophysical properties," Molecules **28**, 1572 (2023).
[35] Y. Xue *et al.*, "An *ab initio* simulation of the UV/visible spectra of substituted chalcones," Open Chem. **8**, 928–936 (2010).
[36] H. Lu, J. Li, T. xue, J. Nie, and X. Zhu, "Substituent effect on the visible light initiating ability of chalcones," Eur. Polym. J. **190**, 111992 (2023).

[37]J. Romand and B. Vodar, "Spectres d'absorption du benzene a l'etat vapeur et a l'etat condense dans l'ultraviolet lointain," Compt. Rend. **233**, 930–932 (1951).
[38]S. F. F. Mason, *UV Atlas of Organic Compounds* (Springer, New York 1967), Vol. 3, p. G1.
[39]S. R. Lemes *et al.*, "Optical properties and antiangiogenic activity of a chalcone derivate," Spectrochim. Acta, Part A **204**, 685–695 (2018).
[40]B. J. Orr and J. F. Ward, "Perturbation theory of the non-linear optical polarization of an isolated system," Mol. Phys. **20**, 513–526 (1971).
[41]J. L. Oudar and D. S. Chemla, "Hyperpolarizabilities of the nitroanilines and their relations to the excited state dipole moment," J. Chem. Phys. **66**, 2664–2668 (1977).
[42]A. M. Kelley, "Frequency-dependent first hyperpolarizabilities from linear absorption spectra," J. Opt. Soc. Am. B **19**(8), 1890–1900 (2002).
[43]J. Pérez-Moreno *et al.*, "Experimental verification of a self-consistent theory of the first-second-and third-order (non)linear optical response," Phys. Rev. A **84**, 033837 (2011).
[44]S. Muhammad, A. G. Al-Sehemi, A. Irfan, and A. R. Chaudhry, "Tuning the push–pull configuration for efficient second-order nonlinear optical properties in some chalcone derivatives," J. Mol. Graphics Modell. **68**, 95–105 (2016).
[45]J. M. F. Custodio *et al.*, "Second-order nonlinear optical properties of two chalcone derivatives: Insights from sum-over-states," Phys. Chem. Chem. Phys. **23**, 6128–6140 (2021).
[46]J. M. F. Custodio *et al.*, "Benzenesulfonyl incorporated chalcones: Synthesis, structural and optical properties," J. Mol. Struct. **1208**, 127845 (2020).
[47]M. G. Kuzyk, "Physical limits on electronic nonlinear molecular susceptibilities," Phys. Rev. Lett. **85**, 1218–1221 (2000).
[48]M. G. Kuzyk, "Fundamental limits on two-photon absorption cross sections," J. Chem. Phys. **119**, 8327–8334 (2003).
[49]A. Cesaretti *et al.*, "Uncovering structure-property relationships in push-pull chromophores: A promising route to large hyperpolarizability and two-photon absorption," J. Phys. Chem. C **124**, 15739–15748 (2020).
[50]Concilio, S. *et al.*, "Third-order nonlinear optical properties of in-backbone substituted oligo(triacetylene) chromophores," J. Opt. Soc. Am. B **20**(8), 1656–1660 (2003).
[51]T. Michinobu *et al.*, "A new class of organic donor–acceptor molecules with large third-order optical nonlinearities," Chem. Commun. **2005**, 737–739.
[52]J. C. May, I. Biaggio, F. Bures, and F. Diederich, "Extended conjugation and donor-acceptor substitution to improve the third-order optical nonlinearity of small molecules," Appl. Phys. Lett. **90**, 251106 (2007).

Studying the First Order Hyperpolarizability spectra in chalcone-based derivatives and the relation with One- and Two-photon absorption transitions

Lucas F. Sciuti[a], Carlos H. D. dos Santos[a], Leandro H. Z. Cocca[a], André G. Pelosi[a], Rafaela G. M. da Costa[b], Jones Limberger[b], Cleber R. Mendonça[a] and Leonardo De Boni[a]

[a] São Carlos Institute of Physics, University of São Paulo, São Carlos 13560-970 São Paulo, Brazil

[b] Departamento de Química, Pontifícia Universidade Católica do Rio de Janeiro. Rua Marquês de São Vicente, 225, 22451-900, Rio de Janeiro, RJ, Brazil

Supplementary Information

1. Open-aperture Z-scan technique

The experimental setup for the open-aperture Z-scan technique measurements consists of an amplified Ti:Sapphire laser (Clark-MXR - CPA) that emits pulses centered at 775 nm, with a temporal width of 150 fs and a repetition rate of 1 kHz. It pumps an OPA (TOPAS - Quantronix) delivering pulses with a spectral range of 460 to 2200 nm. At first, the beam passes in a polarizer and two dielectric mirrors that set the polarization and filter the undesired wavelengths. A spatial filter obtains a Gaussian spatial mode (TEM_{00}). Then, a beam splitter deflects approximately 5% of the incident power to the reference detector. The remaining power passes through a set of polarizers for power control before exciting the sample. A convergent lens of focal length f = 15 cm is used to focus the beam at point z = 0, along which the sample is translated by a motorized translation system (z-axis) controlled by computer software which also performs the data acquisition. After the beam propagates through the sample, it is directed to the signal detector by a convergent lens. Lock-in amplifiers are used in the reference and signal channels for amplification, averaging, and increasing the signal-to-noise ratio. Figure SI-1 shows experimental normalized transmittance (colored circles) for two distinct wavelengths for each studied molecule. The solid lines represent the best fitting of the experimental normalized transmittance (NT) using the theoretical NT given by Eqs. (S1) and (S2).

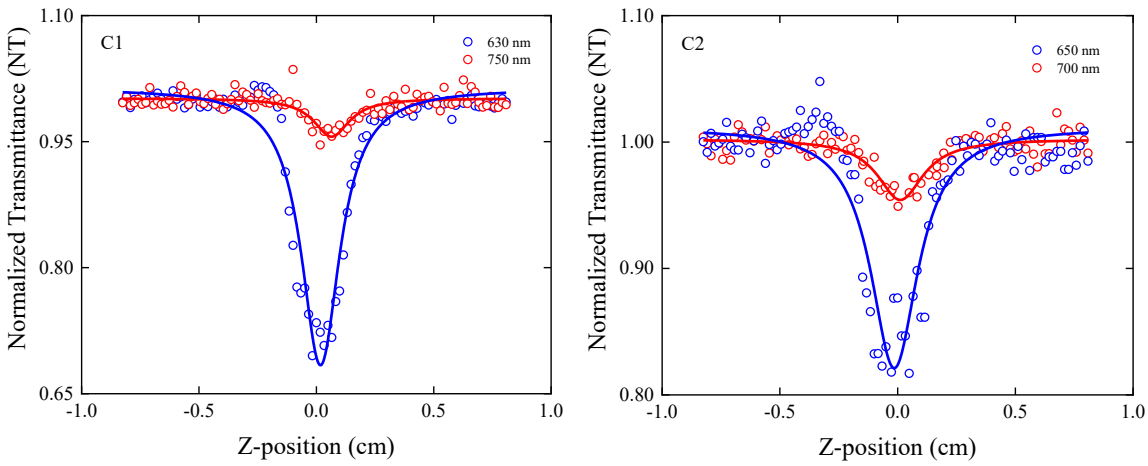

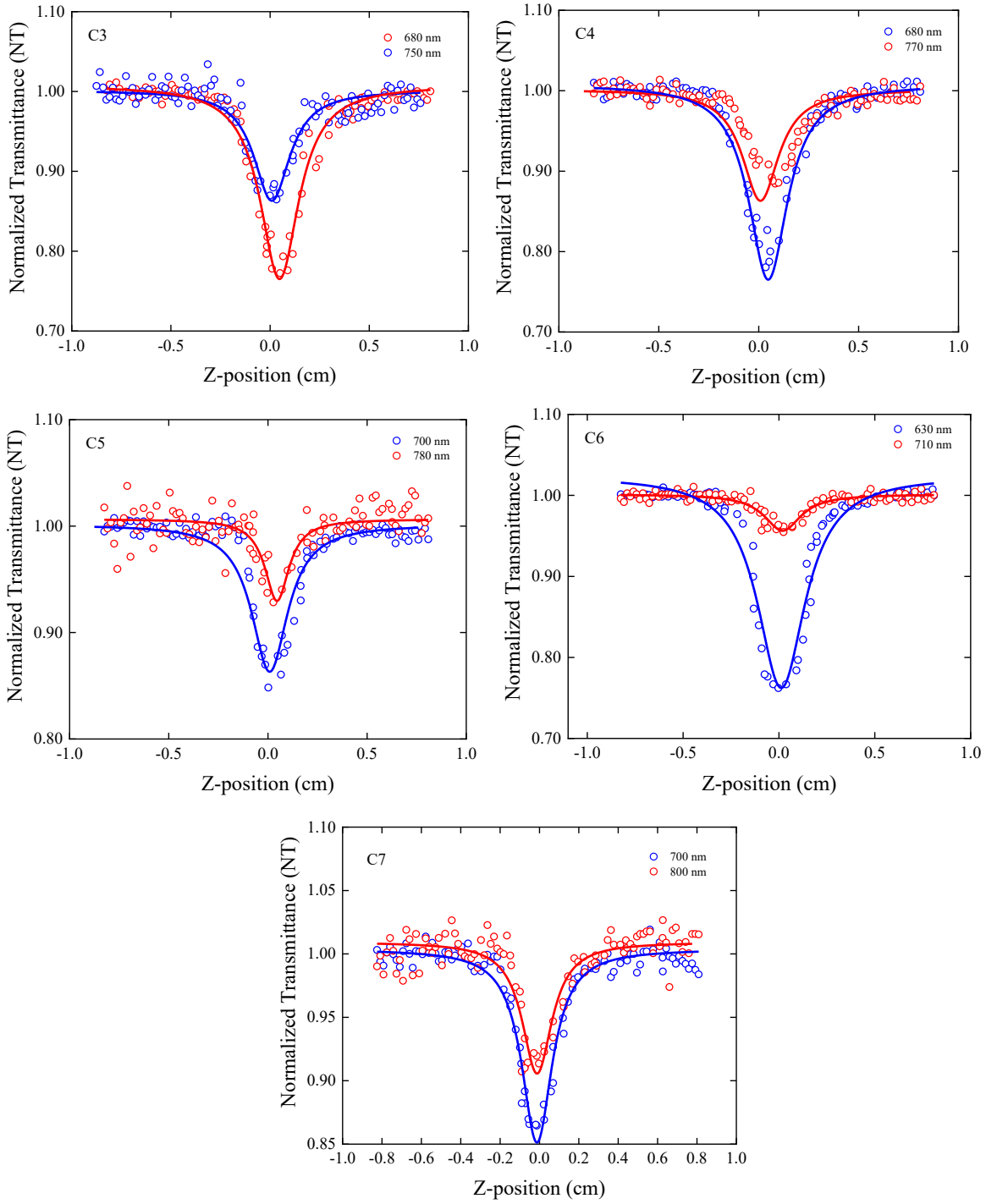

Figure SI-1. Examples of open aperture Z-scan technique for the seven molecules studied. The colored circles were associated with the experimental data and the respective solid lines are the theoretical NT to determine the 2PA cross-section spectra for each wavelength. The pump intensity at the focal plane is around 100 GW/cm^2.

The nonlinear absorption coefficient ζ is determined by fitting the NT curve:

$$NT(z) = \frac{1}{\sqrt{\pi} q_0(z,0)} \int_{-\infty}^{\infty} \ln\left(1 + q_0(z,0) e^{-\tau^2}\right) d\tau \qquad \text{(SI1)}$$

in which,

$$q_0 = \xi I_0 L(1 + (z^2 + z_0^2))^{-1} \quad \text{(SI2)}$$

where L is the sample length, z_0 is the Rayleigh parameter, z is the position of the sample, and I_0 is the intensity of the pulse in the focal plane. The value of the 2PA cross-section, σ_{2PA}, can be obtained by using the expression $\sigma_{2PA} = h\nu\xi/N$, where N is the number of molecules/cm^3 and $h\nu$ is the photon energy. Generally, a 2PA unit is expressed in Göeppert-Mayer (GM), with 1 GM = 10^{-50} cm^4 s molecules^{-1} photon^{-1}.

2. Determining the dispersion of first-order hyperpolarizability by External Reference Method (ERM)

To determine the magnitude of the first-order hyperpolarizability employing ERM, several measurements were performed considering a reference sample (para-nitroaniline (pNA) in this case) with known β values and the chalcone-based derivatives, both dissolved in DMSO. Measurements of I(2ω) as a function of I(ω) were performed for six different concentrations of the reference and the chalcone-based samples, resulting in graphs of $I(2\omega)/I^2(\omega)$ as a function of the concentration. Using the same solvent and experimental conditions for all the molecules, the value of $\beta_{unknown}$ (unknown first-order hyperpolarizability) is given by[1]:

$$\beta_{unknown}(\omega) = \beta_{reference}(\omega)\sqrt{\frac{A_{unknown}}{A_{reference}}} \quad \text{(SI3)}$$

in which $A_{unknown}$ and $A_{reference}$ are, respectively, the slopes of the linear fits of the quadratic coefficients ($I(2\omega)/I^2(\omega)$) as a function of the concentrations.

As an example of a typical HRS experimental curve, in Figure SI-2 (a), one can see the quadratic dependence of I(2ω) with I(ω) for six C3 concentrations, measured with an incident laser beam at 800 nm. In addition, in Fig. SI-2 (b), the quadratic coefficients ($I(2\omega)/I^2(\omega)$) are plotted as a function of both C3 and pNA concentrations, showing the expected linear behavior where the linear fits (solid lines) slopes are obtained. The measurements were performed over wavelengths ranging from 750 nm to 1200 nm with 50 nm intervals and the values of β(λ) for pNA were obtained from Sciuti et al[2].

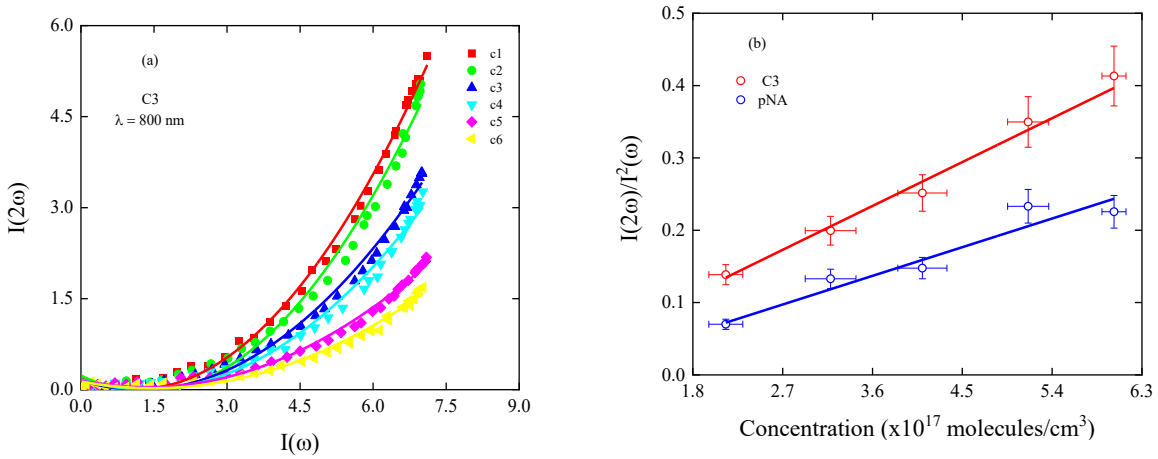

Figure SI-3 - (a) indicates one example of the measurements of I(2ω) vs I(ω) and their respective quadratic fits for molecule C3 as a function of concentration, measured at 800 nm, in which C1 is the most concentrated solution. (b) depicts the linear dependence of the quadratic coefficient with sample concentration for pNA, C3, at the same wavelength. Both error bars were estimated at 10%, which is considered the concentration error and laser power fluctuation.

References

[1] R.D. Fonseca, M.G. Vivas, D.L. Silva, G. Eucat, Y. Bretonnière, C. Andraud, L. De Boni, and C.R. Mendonça, "First-Order Hyperpolarizability of Triphenylamine Derivatives Containing Cyanopyridine: Molecular Branching Effect," Journal of Physical Chemistry C **122**(3), 1770–1778 (2018).

[2] L.F. Sciuti, L.M.G. Abegão, C.H.D. dos Santos, L.H. Zucolotto Cocca, R.G.M. da Costa, J. Limberger, L. Misoguti, C.R. Mendonça, and L. De Boni, "Modeling the First-Order Molecular Hyperpolarizability Dispersion from Experimentally Obtained One- and Two-Photon Absorption," The Journal of Physical Chemistry A **126**(14), 2152–2159 (2022).